Synthesis and Reactivity of Mercury-Bridged Transition-Metal Clusters. 4.[1a] Reactivity of $(\mu_3\text{-}\eta^2\text{-}C_2\text{-}t\text{-}Bu)(CO)_9Ru_3HgMo(\eta^5\text{-}C_5H_5)(CO)_3$

Edward Rosenberg* and Jiandang Wang

Department of Chemistry, California State University, Northridge, California 91330

Robert W. Gellert

Department of Chemistry, California State University, Los Angeles, California 90032

Received August 3, 1987

The thermolysis, photolysis, and phosphine substitution reactions of $[Ru_3(\mu_3\text{-}\eta^2\text{-}C_2\text{-}t\text{-}Bu)(CO)_9](\mu_3\text{-}Hg)[Mo(\eta^5\text{-}C_5H_5)(CO)_3]$ (I) and its derivatives have been studied. Redistribution reaction between the two different monophosphine-substituted derivatives of I show that the Hg–Mo bond is relatively labile compared to the μ-Hg–Ru_2 bond. Photolysis of I yields the product $(\mu_3\text{-}\eta^2\text{-}C_2\text{-}t\text{-}Bu)Ru_2Mo(\eta^5\text{-}C_5H_5)(CO)_8$ (VII), a new triangular mixed-metal cluster. The solid-state structure of VII was determined by X-ray crystallography. Compound VII crystallizes in the monoclinic space group $P2_1/c$ with a = 9.116 (2) Å, b = 15.982 (3) Å, c = 13.510 (5) Å, β = 108.81 (2)°, V = 2139.1 (8) Å^3, and d_{calcd} = 2.075 g/cm^3 for Z = 4. Least-squares refinement led to final agreement indices R = 0.018 and R_w = 0.024 for 3217 observed reflections. An investigation of the ligand dynamics of VII by variable-temperature ^{13}C NMR revealed that there is no intermetallic scrambling of carbonyls around the Ru_2Mo triangle, but a restricted edge-hopping motion of the coordinated acetylide between the two Ru–Mo edges is observed.

Introduction

We have been studying the synthesis and reactivity of mercury-mixed transition-metal clusters.[2-4] One of the goals of this research is to elucidate the fundamental differences between the well-known two-center, two-electron mercury–transition-metal bond and the more recently reported μ-, μ_3-, and μ_4-electron-deficient transition metal–mercury bonds. We recently reported the results of such a study comparing the chemistry of $[(\mu_3\text{-}\eta^2\text{-}C_2\text{-}t\text{-}Bu)(CO)_9Ru_3]_2(\mu_4\text{-}Hg)$ (II) with M–Hg–M (M = transition metal) systems.[4] We report here a related study on the compound $[(\mu_3\text{-}\eta^2\text{-}C_2\text{-}t\text{-}Bu)(CO)_9Ru_3](\mu_3\text{-}Hg)[Mo(\eta^5\text{-}C_5H_5)(CO)]_3$ (I) where a comparison of the normal covalent

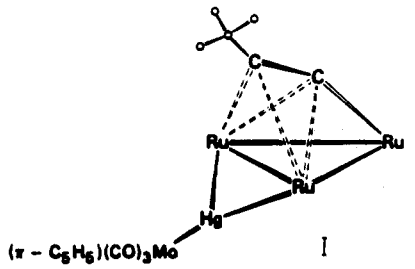

I

and electron-deficient mercury transition-metal bonds can be compared in the same molecule. A second goal of this research is to utilize the known photoreactivity of mercury to synthesize heterometallic bonds by photoinduced reductive elimination of mercury. While we previously found II to be photochemically inactive,[4] we report here that I undergoes not only an apparent elimination of mercury but also a regiospecific replacement of one Ru atom by the Mo atom in the original Ru_3 triangle of I.

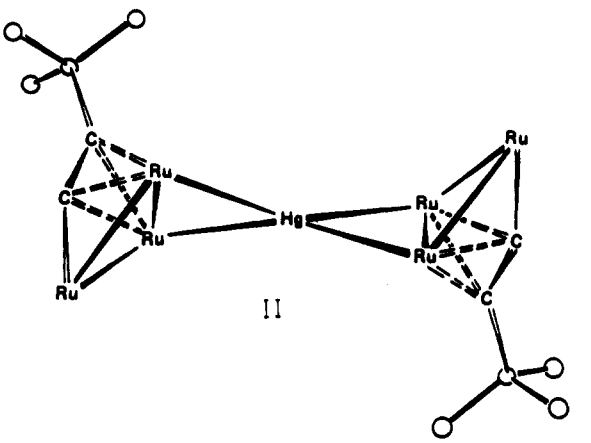

II

Results and Discussion

A. Thermolysis of I. $[Ru_3(\mu_3\text{-}\eta^2\text{-}C_2\text{-}t\text{-}Bu)(CO)_9](\mu_3\text{-}Hg)[Mo(\eta^5\text{-}C_5H_5)(CO)_3]$ (I) is relatively stable toward thermal decomposition. Nevertheless, refluxing I in solvents of boiling point lower than 100 °C under N_2 atmosphere for 20 h resulted in the formation of some $H[Ru_3(\mu_3\text{-}\eta^2\text{-}C_2\text{-}t\text{-}Bu)(CO)_9]$, II,[2] and $Hg[(Mo(\eta\text{-}C_5H_5)(CO)_3]_2$ (III),[5] each of which was identified by TLC, IR, and ^1H NMR (eq 1). From the yield data shown in eq 1, two

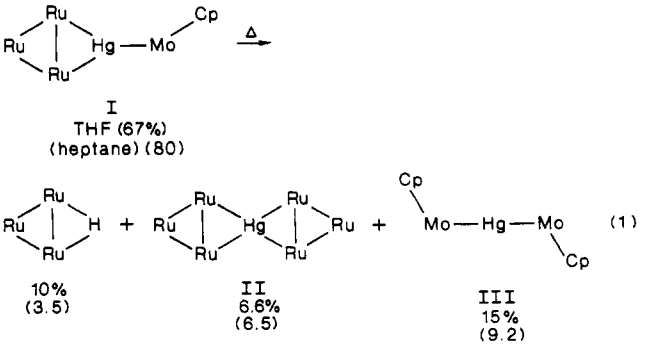

(1) (a) For parts 1–3 see ref 2–4 below. (b) Rosenberg, E.; King, K.; Fahmy, R.; Tiripicchio, A. *J. Am. Chem. Soc.* **1980**, *102*, 3626.
(2) Rosenberg, E.; Hardcastle, K.; Ermer, S.; King, K.; Tiripicchio, A. *Inorg. Chem.* **1983**, *22*, 1339.
(3) Rosenberg, E.; Ryckman, D.; Gellert, R.; Hsu, I. *Inorg. Chem.* **1986**, *25*, 194.
(4) (a) Novak, B. Masters Thesis, California State University, Northridge. (b) Rosenberg, E.; Novak, B. *Organometallics*, submitted for publication.

(5) Mays, M. J.; Pearson, S. M. *J. Chem. Soc. A* **1968**, *68*, 2291.

0276-7333/88/2307-1093$01.50/0

Table I. Spectroscopic and Analytical Data for Compounds Reported

	I	IV	V	VI	VII
mol mass	1082.10	1316.38	1316.38	1550.66	668.39
infrared (methylene chloride) (cm^{-1})					
(-C≡O)	2075 (w)	2085.5 (w)	2079.5 (m)	2055.1 (m)	2071.9 (s)
	2025 (s)	2080.8 (w)	2050.0 (s)	2035.3 (s)	2037.0 (s)
	1993 (s)	2053.7 (m)	2043.7 (s)	1998.2 (s)	2000.3 (s)
	1985 (s)	2040.8 (s)	2007.8 (s)	1986.5 (s)	1967.6 (m)
	1915 (m)	2001.3 (s)	1888.5 (w)	1966.0 (m)	1903.9 (w)
	1890 (s)	1936.0 (w)	1824.2 (m)	1936.0 (w)	
		1906.5 (m)		1886.5 (w)	
		1881.9 (m)		1821.2 (m)	
		1821.0 (w)			
^1H NMR (chloroform-*d*) (ppm)					
$-CH_3$	1.40 (9, s)	1.42 (9, s)	1.40 (9, s)	1.42 (9, s)	1.41 (8, s)
$-C_5H_5$	5.29 (5, s)	5.33 (5, s)	4.92 (5, d)	4.93 (5, d)	5.34 (5, s)
$-C_6H_5$		7.44 (15, m)	7.38 (15, m)	7.41 (15, m)	
^{31}P NMR (chloroform)[a] (ppm)					
(Mo)-PPh_3			81.42 (s)	81.74 (1 P, s)	
(Ru)-PPh_3		64.80 (s)		64.85 (1 P, s)	
mass spectra (amu)					
mol ion	1082				668
elemental analysis (%)					
found C	25.87	36.80	36.62	43.85	34.19
found H	1.74	2.26	2.36	2.99	1.01
calcd C	25.53	36.50	36.50	44.15	34.14
calcd H	1.50	2.22	2.22	2.86	0.91

[a] ^{31}P NMR chemical shifts are reported downfield positive relative to external 85% H_3PO_4 (uncorrected for bulk susceptibility).

points can be made: first, a larger percent of the starting material decomposes, overall, in tetrahydrofuran than in heptane despite the fact that heptane has a boiling point 31 degrees higher than that of THF; second, the yield of the hydrido cluster is lower than that of II in the heptane reaction whereas the yield of II is lower in the THF reaction. Redistribution reactions involving homolytic and heterolytic bond cleavages and/or bimolecular intermediates could lead to the formation of II and III. Although products assignable to cleavage of both types of Hg–metal bonds in I are observed, their relative rate of cleavage is not revealed by these experiments. The formation of the hydrido cluster suggests the formation of Ru_3 radicals that then abstract hydrogen from the solvent.

B. Phosphine Substitution Reactions on I. Triphenyl, trimethyl, and other phosphines substitute for one or two CO ligands in compound II with relative ease.[4] Starting material was usually consumed within a few hours. The phosphine substitutes for one carbonyl on the wing-tip Ru atom in one triangle of II to form a monosubstituted product followed by a second substitution on the analogous Ru atom of the second triangle in refluxing toluene. $[Mo(\eta^5\text{-}C_5H_5)(CO)_3]_2Hg$ (III) also readily undergoes bis(phosphine) substitution at each Mo atom.[5]

When a solution of I is refluxed with triphenyl- or trimethylphosphine at 65–100 °C, two different mono(phosphine)-substituted derivatives of I are observed to be the initial products formed. These products, IV and V, have R_f (TLC, silica gel) values very close to one another and were difficult to separate. Both products (IV and V) show ^1H NMR resonances for the *tert*-butyl methyl groups, the cyclopentadienyl group, and the alkyl or aryl groups of the phosphine ligand in a 1:1:1 stoichiometric ratio (see Table I). The chemical shifts of analogous resonances were different for IV and V. The product with a greater R_f value (V) has a cyclopentadienyl resonance that appears as a doublet (J = 1.1 Hz). This is assigned to a three-bond proton–phosphorus coupling, suggesting that in this isomer, the phosphine is bound to the Mo atom.[6] Product IV, on the other hand, has a singlet resonance for its cyclopentadienyl group. The ^{31}P NMR spectrum for V shows a single peak at 81.42 ppm (with respect to H_3PO_4, δ 0) and two Hg satellites arising from a Hg–P two-bond coupling ($^2J(^{199}Hg\text{–}^{31}P)$ = 278 Hz). IV also gave a singlet in its ^{31}P NMR spectrum at 64.80 ppm but with no satellites. The latter chemical shift is identical with that observed for mono- or *bis*-substituted phosphine derivatives of II where the phosphine substitutes on one (64.89 ppm) or both (64.51 ppm) of the wing-tip rutheniums, respectively.[4] When a phosphine substitutes on one of the ruthenium atoms bridged to the Hg in II, the ^{31}P NMR resonance was found at 44.89 ppm with two mercury satellites due to the two-bond coupling ($^2J(^{199}Hg\text{–}^{31}P)$ = 573.6 Hz).[4] Therefore, the phosphine is substituted on the wing-tip ruthenium atom in IV and on the molybdenum atom in V. At longer reaction times, a low R_f product, VI, is observed. The ^1H NMR of this product shows a relative intensity of 30:9 for the phenyl and *tert*-butyl methyl protons, respectively. The ^{31}P NMR spectrum contained two resonances of equal intensity at 64.85 (no satellites) and 82.74 ppm ($^2J(^{199}Hg\text{–}^{31}P)$ = 271 Hz). This leaves no doubt that VI is a *bis*(phosphine) substitution product of I where one phosphine substitutes on each metal moiety (eq 2). Attempts

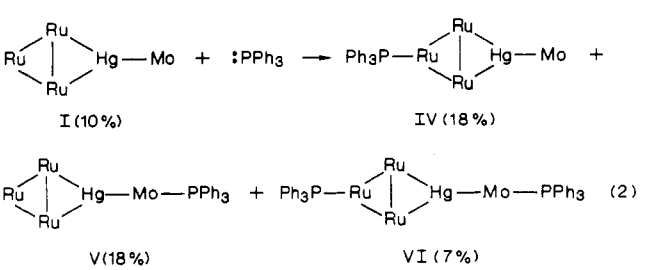

(2)

to improve the yields of IV, V, and VI and the percentage of conversion of the starting material were unsuccessful. We were unable to find conditions where all the starting material was consumed. Varying the basicity of phosphine, the amount of phosphine, or the temperature did not significantly affect the conversion rate. Temperature increased the reaction rate, as expected. The best yields of

(6) Kubicki, M. M.; Kergoat, R.; Gall, J. X. L.; Guerchais, J. E.; Douglade, J. *Aust. J. Chem.* **1982**, *35*, 1343.

Table II. K_{eq}'s and Equilibration Times for Redistribution Reactions

eq	type	equilibration time	K_{eq}
3	MHgM + XHgX ⇌ 2 MHgX	few min	>1000
7	M_3HgM' + $'M_3HgM$ ⇌ M_3HgM + $'M_3HgM'$	1–2 h	0.43
5	M_2HgM_2 + XHgX ⇌ 2 M_2HgX	36 h	>100
6	M_3HgX ⇌ M_3HgM_3 + XHgX	28–31 days	0.5–0.8

Table III. Crystal Data: Collection and Refinement Parameters

formula	$Ru_2Mo(CO)_8(\eta^5\text{-}C_5H_5)(\mu_3\text{-}C_2C(CH_3)_3)$
fw	668.40
cryst system, space group	monoclinic, $P2_1/c$
a, Å	9.116 (2)
b, Å	15.982 (3)
c, Å	15.510 (5)
β, deg	108.81 (2)
V, Å^3	2139.1 (8)
Z	4
d_{calcd}, g/cm^3	2.075
cryst size, mm	0.22 × 0.32 × 0.40
radiatn (λ, Å)	Mo Kα (0.71069)
abs coeff, μ (cm^{-1})	19.73
scan range, deg	$2.5 < 2\theta \leq 50$
scan speed, deg/min	1.0–19.0 (ω-scan)
ratio bkgd/scan time	0.5
no. of data collcd	4142 ($+h,+k,\pm l$)
no. of observns [$F_o^2 > 3\sigma(F_o^2)$]	3217
no. of variables	313
R^a	0.018
$R_w{}^b$	0.024
GOF^c	0.99
largest peak, e/Å^3	0.32
largest Δ/σ, final cycle	0.29

$^a R = \sum(|F_o| - |F_c|)/\sum|F_o|$. $^b R_w = [\sum w(|F_o| - |F_c|)^2/\sum w|F_o|^2]^{1/2}$. ^{c}GOF $= [\sum w|F_o| - |F_c|)^2/(N_{observns} - N_{parameters})]^{1/2}$.

IV and V were obtained with reaction times of about 36 h.

Redistribution Reactions of IV and V. There have been a number of studies reported on the redistribution reactions of mercury–transition-metal bonds in compounds of the type L_nMHgX (L = CO, PPh_3, η^5-C_5H_5, CNR, and sulfur donors; M = Cr, Mo, W, Mn; X = halides, pseudohalides, alkyl or aryl groups, or another metal ligand). The position of equilibrium (eq 3) lies far to the right for

$$HgX_2 + M_2Hg \rightleftharpoons 2MHgX \quad (3)$$

X = halide and far to the left for X = alkyl or aryl.[5,6] When $[Mo(\eta^5\text{-}C_5H_5)(CO)_3]_2Hg$ was mixed with equimolar mercuric halide, HgX_2, the equilibrium was established very rapidly and no trace of the symmetrical mercurial could be detected in the equilibrium mixture.[5] Redistribution between mixed-metal clusters containing three-center, two-electron mercury–transition-metal bonds such as $Ph(\mu\text{-}Hg)Mn_2(\mu\text{-}PPh_2)(CO)_8$ or $Cl(\mu\text{-}Hg)Mn_2(\mu\text{-}PPh_2)(CO)_8$ and $(\mu_4\text{-}Hg)[Mn_2\text{-}\mu\text{-}PPh_2(CO)_8]_2$ favored the symmetrical mercurial over the unsymmetrical one in the case of phenylmercurial and the unsymmetrical over the symmetrical in the case of chloromercurial (eq 4 and 5).

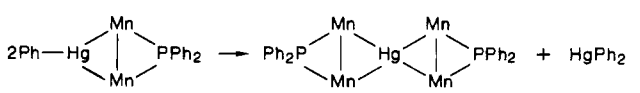

(4)

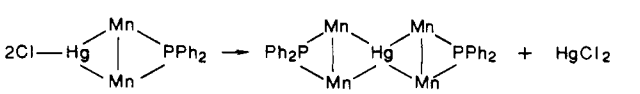

(5)

The compounds $[(\mu_3\text{-}\eta^2\text{-}C_2\text{-}t\text{-}Bu)(CO)_9Ru_3](\mu\text{-}HgX)$ (X = Br, I) redistribute to give II and HgX_2 extremely slowly and yield an equilibrium mixture containing comparable amounts of the symmetrical and unsymmetrical species (eq 6).[3] The reason why the phosphine substitution re-

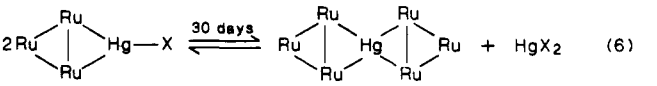

II

$K_{eq} = 0.5 - 0.8$

actions of I do not go to completion can be rationalized by an operative redistribution reaction. When solutions of IV (the mono(triphenylphosphine)-substituted I in which the phosphine is on the rutheniums) and V (also mono-substituted I but with the phosphine on the molybdenum) are mixed, they rapidly redistribute into the unsubstituted (I) and the bis-substituted (VI) species (eq 7) at *room temperature*. The reaction reached equilib-

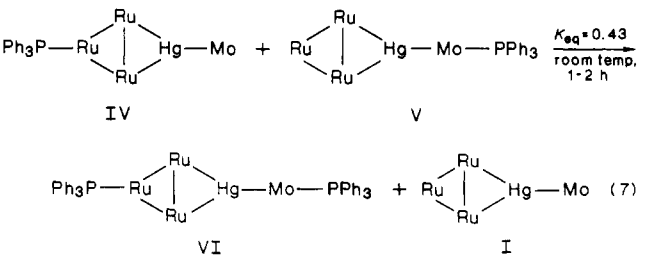

rium within 2 h, which represents an intermediate rate for a mercury redistribution reaction slower than the MHgX redistribution (in eq 3) but faster than the redistribution of II (eq 6) (Table II). The equilibrium constant, K_{eq}, for eq 7 is 0.43, as estimated from integration of ^{1}H NMR resonances arising from the *tert*-butyl groups in the molecules involved in the reaction. This K_{eq} value is much smaller than those for reactions 3 and 5 but about the same as that for reaction 6.

It is well-known that once substituted onto a metal, a phosphine ligand dissociates relatively slowly. The cleavage and reformation of the Hg–Mo bond causes the redistribution of IV and V to I and VI. The fact that no formation of double cluster II and no III or hydrido cluster was observed for at least 24 h after mixing of IV with V clearly indicates that either the Hg–Mo bond or the μ-Hg–Ru_2 bond is being cleaved rapidly, but not both. Our previous study of the redistribution reactions of a phosphine-substituted derivative of II showed that redistribution rates in these μ_4-Hg clusters are much slower (equibration in 11 h at 100 °C) than for IV and V.[4] This leads one to the conclusion that the Hg–Mo bond in IV and V is much more labile than the μ-Hg–Ru_2 bond. Cleavage of this bond could occur by either homolytic or heterolytic cleavage of the Hg–Mo. The latter possibility is precluded by the fact that no formation of $HMo(\eta\text{-}C_5H_5)(CO)_3$ is observed when either I, IV, V, or VI is treated with excess trifluoroacetic acid. Only protonation of the Ru_3 moiety in these complexes is observed (see Experimental Section). If heterolysis of the Hg–Mo bond were occurring, the formation of $HMo(\eta\text{-}C_5H_5)(CO)_3$ would be expected. The redistribution reaction in eq 7 must therefore occur by either a homolytic dissociative pathway or an associative bimolecular pathway. Naturally, at this point we cannot ascertain what influence, if any, the

(7) Iggo, J. A.; Mays, J. *J. Chem. Soc., Dalton Trans.* **1984**, *84*, 643.

Table IV. Selected Bond Distances (Å) and Angles (deg) with Their Estimated Standard Deviations for VII

(a) In the Coordination Sphere of the Metal Atoms

Mo–Ru(1)	2.8290 (3)	Ru(1)–C(11)	1.921 (3)	Mo–C(1)	2.248 (3)	Mo–C(7)	2.339 (4)
Ru(1)–Ru(2)	2.7831 (3)	Ru(1)–C(12)	1.904 (4)	Mo–C(2)	2.330 (2)	Mo–C(8)	2.315 (4)
Ru(2)–Mo	2.9227 (3)	Ru(1)–C(13)	1.888 (4)	Ru(1)–C(1)	2.209 (3)	Mo–C(9)	2.313 (4)
Mo–C(31)	1.978 (3)	Ru(2)–C(21)	1.918 (4)	Ru(1)–C(2)	2.234 (3)	Mo–C(10)	2.336 (4)
Mo–C(32)	1.994 (3)	Ru(2)–C(22)	1.907 (4)	Ru(2)–C(1)	1.964 (3)	Mo–C(14)	2.366 (4)
Ru(1)–C(31)	2.892 (3)	Ru(2)–C(23)	1.895 (3)				

Ru(1)–Mo–Ru(2)	57.849 (8)	Ru(2)–Ru(1)–Mo	62.763 (8)	Ru(1)–Ru(2)–Mo	59.388 (8)
C(32)–Mo–Ru(1)	78.9 (1)	C(12)–Ru(1)–Mo	106.9 (1)	C(21)–Ru(2)–Mo	107.0 (1)
C(32)–Mo–Ru(2)	75.0 (1)	C(12)–Ru(1)–Ru(2)	90.2 (1)	C(21)–Ru(2)–Ru(1)	102.3 (1)
C(31)–Mo–Ru(1)	71.5 (1)	C(11)–Ru(1)–Mo	111.0 (1)	C(22)–Ru(2)–Mo	152.8 (1)
C(31)–Mo–Ru(2)	127.9 (1)	C(11)–Ru(1)–Ru(2)	173.3 (1)	C(22)–Ru(2)–Ru(1)	99.8 (1)
		C(13)–Ru(1)–Mo	146.1 (1)	C(23)–Ru(2)–Mo	101.4 (1)
		C(13)–Ru(1)–Ru(2)	91.2 (1)	C(23)–Ru(2)–Ru(1)	158.0 (1)

(b) In the Carbonyl Groups

C(31)–O(31)	1.143 (4)	C(11)–O(11)	1.137 (4)	C(21)–O(21)	1.139 (5)	C(13)–O(13)	1.139 (5)
C(32)–O(32)	1.146 (4)	C(12)–O(12)	1.130 (5)	C(22)–O(22)	1.129 (5)	C(23)–O(23)	1.133 (5)

(c) In the Organic Ligands

C(1)–C(2)	1.304 (4)	C(3)–C(4)	1.537 (5)	C(7)–C(8)	1.384 (6)	C(10)–C(14)	1.384 (6)
C(2)–C(3)	1.511 (4)	C(3)–C(5)	1.528 (5)	C(8)–C(9)	1.410 (5)	C(14)–C(7)	1.393 (6)
		C(3)–C(6)	1.532 (5)	C(9)–C(10)	1.406 (5)		

Ru(2)–C(1)–C(2)	154.6 (2)	C(2)–C(3)–C(5)	112.2 (2)	C(14)–C(7)–C(8)	108.5 (3)
Ru(1)–C(1)–Mo	78.80 (9)	C(2)–C(3)–C(6)	108.0 (3)	C(7)–C(8)–C(9)	108.1 (3)
Ru(1)–C(2)–Mo	76.58 (8)	C(4)–C(3)–C(5)	109.1 (3)	C(8)–C(9)–C(10)	106.7 (3)
Ru(2)–C(1)–Ru(1)	83.4 (1)	C(4)–C(3)–C(6)	109.2 (3)	C(8)–C(9)–Mo	72.3 (2)
Ru(2)–C(1)–Mo	87.6 (1)	C(5)–C(3)–C(6)	109.2 (3)	C(10)–C(9)–Mo	73.3 (2)
C(1)–C(2)–C(3)	144.1 (3)	C(9)–C(10)–C(14)	108.6 (3)	C(9)–Mo–Ru(1)	141.70 (9)
C(2)–C(3)–C(4)	109.1 (2)	C(7)–C(14)–C(14)	108.0 (3)	C(9)–Mo–Ru(2)	132.84 (9)

presence of the phosphine ligand on the Mo atom in IV has on this process.

C. Photolysis of I. When I is irradiated (Pyrex-filtered 125-Watt Hg Hanovia lamp) in benzene, it undergoes the photochemical reaction shown in eq 8. All minor side

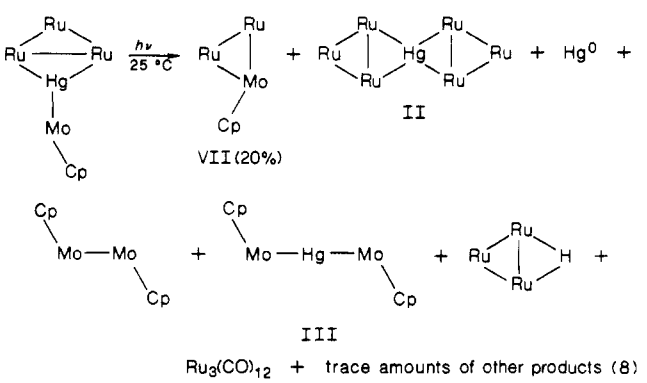

products have not been identified, but $(\mu_3\text{-}\eta^2\text{-}C_2\text{-}t\text{-}Bu)Ru_2Mo(\eta^5\text{-}C_5H_5)(CO)_8$ (VII) is the major product for which the yield was 20%. None of the other products are isolated in higher yield than 7%. Compound VII was identified by an X-ray crystallographic investigation (see below). This reaction is the first example of inserting a metal atom into the otherwise stable cluster moiety $(\mu_3\text{-}\eta^2\text{-}C_2\text{-}t\text{-}Bu)Ru_3(CO)_9$.[2-4] The reaction further demonstrates the greater reactivity of the two-center, two-electron Hg–Mo bond over the μ-Hg–Ru_2 bond, since it has been shown that the μ_4-mercury-bridged double cluster II is photochemically inert under identical reaction conditions.[4] As a control, we tried to photochemically react $[Mo(\eta^5\text{-}C_5H_5)(CO)_3]_2$ with $H[Ru_3(\mu_3\text{-}\eta^2\text{-}C_2\text{-}t\text{-}Bu)(CO)_9]$ and no reaction took place except for some decomposition of the molybdenum dimer. The presence of the mercury bridge, therefore, is essential to this photochemical reaction.

Although further study is necessary to elucidate the mechanistic sequence of the reaction to form VII, it is fairly safe to assume that the first step of the reaction involves

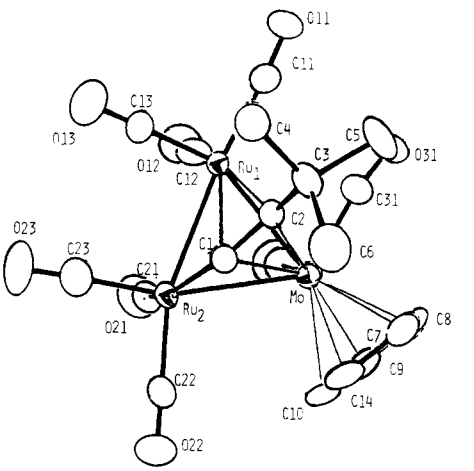

Figure 1. Solid-state structure of VII showing atomic numbering system.

the dissociation of Hg–Mo bond to form the radicals $[Ru_3(\mu_3\text{-}\eta^2\text{-}C_2\text{-}t\text{-}Bu)(CO)_9]\text{-}\mu\text{-}Hg^\bullet$ and $^\bullet[Mo(\eta^5\text{-}C_5H_5)(CO)_3]$, since we know from our redistribution reaction studies that the homolytic dissociation of the Hg–Mo bond is a facile process in solution. Further studies are under way to determine the mechanism of this reaction.

D. Crystal Structure of VII. The solid-state structure of $(\mu_3\text{-}\eta^2\text{-}C_2\text{-}t\text{-}Bu)Ru_2Mo(\eta^5\text{-}C_5H_5)(CO)_8$ (VII) with the atomic numbering system is presented in Figure 1, selected bond distances and angles are given in table IV. In the Ru_2Mo triangle, the Ru–Ru bond (2.7831 (3) Å) is substantially shorter than both Ru(1)–Mo and Ru(2)–Mo bonds (2.8292 and 2.9227 (3) Å, respectively) and is also shorter than the corresponding Ru–Ru bonds in I (2.812 (2) and 2.818 (2) Å). Of the eight CO groups, five (two on each Ru and one on Mo) are approximately equatorial with regard to the plane of the metallic triangle and three (one on each metal atom) are axial.

While the *tert*-butyl fragment of the *tert*-butylacetylido group points away from the Ru_2Mo plane (bond angle

C(1)–C(2)–C(3) = 144.1 (3)°), the C(1)–C(2) alkyne fragment coordinates to all three metal atoms in a μ_3-η^2 fashion. It sits on top of the Ru(1)–Mo edge of the metal triangle with an orientation perpendicular to the Ru(1)–Mo bond and the C(1) atom pointing in toward the Ru(2) tip. The Ru(2)–C(1) distance is the shortest, 1.964 (3) Å as opposed to 2.209 (3) and 2.234 (3) Å from Ru(1) and 2.248 (3) and 2.330 (2) Å from Mo to C(1) and C(2), respectively. Both the bond distance and the orientation indicate that in this structure the organic group formally σ-bonds through C(1) to one of the ruthenium atoms, Ru(2), not to the heteroatom Mo. As a result, the Mo atom has a local electron count of 19 in its coordination sphere whereas Ru(1) and Ru(2) have 18 and 17, respectively, according to the EAN formalism. If the C_2-*t*-Bu group did σ-bond to Mo, the molecule would, in fact, be more electron precise with each metal atom having 18 electrons. It is notable that a similar asymmetric trimetallic cluster, (μ_3-η^2-C_2-*t*-Bu)$Fe_2Ni(\eta^5$-$C_5H_5)(CO)_6$, exists, where the Ni atom has 19 electrons and the corresponding iron atoms have 17 and 18 electrons.[8] The origin of this structural pattern is not clear, but it does not seem to be steric since the more symmetrical structure would decrease crowding between the bulky *tert*-butyl group and the cyclopentadienyl group. The angle between the plane defined by the five carbon atoms of the Cp ring and the one defined by the three metal atoms is 78.1 (1)°, with the Cp ring tilted toward the *tert*-butylacetylene group. The geometry around the Mo atom is intermediate between a square-based pyramid and a trigonal bipyramid. Looking down the axis which goes through the centroid of the Cp ring and the molybdenum atom, Ru(2), C(31), C(32), C(2), and Mo form a distorted square-based pyramid, while C(31), C(32), and C(1) with Ru(1) and Mo form a trigonal bipyramid.

E. Variable-Temperature ^{13}C NMR of VII in Solution. The ^{13}C NMR spectrum of a ^{13}CO-enriched sample of VII at −75 °C in CD_2Cl_2 shows eight resonances of approximately equal intensity at 224.85, 224.44, 202.84, 201.29, 196.33, 195.40, 193.77, and 193.26 ppm as expected from the solid-state structure in which no two of the eight CO's are equivalent (Figure 2). As the temperature is increased, the six upfield resonances (196.3–193.3 ppm) assigned to the carbonyl groups on the two rutheniums begin to broaden. At 0 °C, two peaks were seen at 197.43 and 196.85 ppm for the ruthenium carbonyls, the former sharp and the latter broad. These two are the result of independent local axial–radial exchange on the two rutheniums, for their chemical shifts are the exact numerical averages of two sets of three peaks in the −75 °C spectrum. The axial CO resonance at 202.84 ppm averages with the two radial CO resonances at 196.33 and 193.26 ppm to give rise to the sharp 197.43 ppm peak; and the 201.29, 195.40, and 193.77 ppm resonances average to the broad resonance at 196.85 ppm. When the temperature is increased to 30 °C, the two molybdenum–carbonyl resonances began to average and simultaneously the two ruthenium resonances began to average with each other. At this stage of the experiment, the solvent was changed from CD_2Cl_2 to $C_6D_5CD_3$, and the spectrum obtained at 30 °C from this solution also had four separate but broad resonances at 224.46, 224.2, 197.66, and 196.66 ppm (Figure 2). At 100 °C, two sharp peaks remained at 224.31 and 197.36 ppm, one for the two molybdenum carbonyls and the other for the six carbonyls on the two ruthenium atoms. However, the intensity ratio between these two peaks is smaller than 1:3 because of the different levels of enrichment at the Mo and the Ru centers. The sharpness and separation of these two peaks as well as the preservation of the different levels of enrichment excludes intermetallic scrambling of CO's at this temperature. The absence of intermetallic CO scrambling is very likely due to the presence of the bulky cyclopentadienyl group, an η^5-ligand perpendicular to the plane of the Ru_2Mo triangle, which evidently blocks off the pathway by preventing the formation of carbonyl bridges at all three metal edges, a prerequisite for intermetallic CO scrambling. In order for carbonyl exchange to take place between any two edges, two CO bridges would have to form in the intermediate. This seems very unlikely in a metal triangle where one face is already bridged by the organic ligand. To account for the simultaneous averaging of the CO's at Ru(1) with the CO's at Ru(2) and the two CO's on the molybdenum with each other we propose that, at elevated temperatures, the *tert*-butylacetylido group rapidly changes its position from one Ru–Mo edge to the other Ru–Mo edge of the Ru_2Mo triangle, undergoing an "edge-hopping" process (Figure 3). The configuration around the molybdenum atom is intermediate between a square-based pyramid and a trigonal bipyramid. Since square-based pyramid to trigonal bipyramid interconversion is known to be a facile process,[9] the energy barrier for the required ligand motions in such an "edge-hopping" process could be accessible. As the *tert*-butylacetylido group moves from one edge to the other, the cyclopentadienyl ring formally switches its position, or "swings", to the opposite side of the Mo atom. Although we cannot say which individual ligands actually

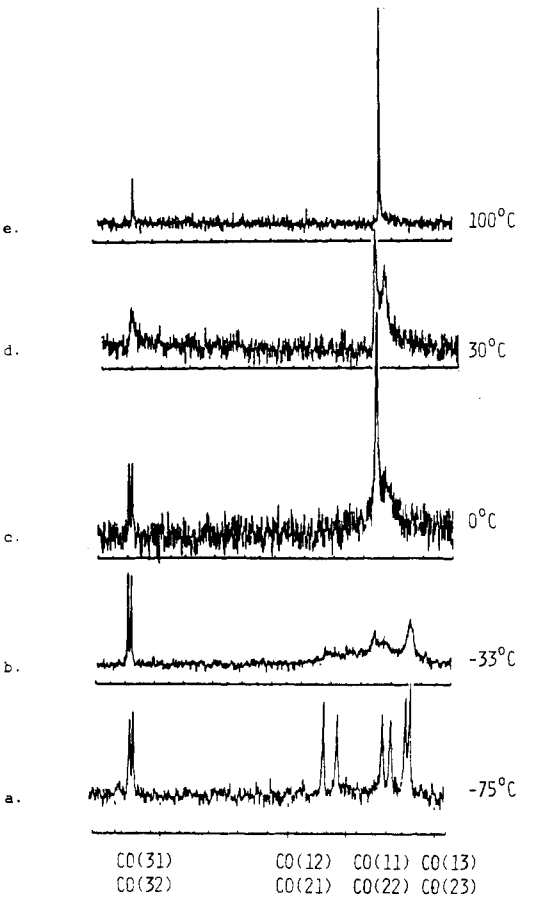

Figure 2. Variable-temperature ^{13}C NMR of VII at 20.4 MHz in CD_2Cl_2.

(8) Martinetti, A.; Sappa, E.; Tiripicchio, A.; Camellini, M. T. *J. Organomet. Chem.* **1980**, *197*, 335.

(9) Flood, T. C.; Rosenberg, E.; Sirhangi, A. *J. Am. Chem. Soc.* **1977**, *99*, 4334.

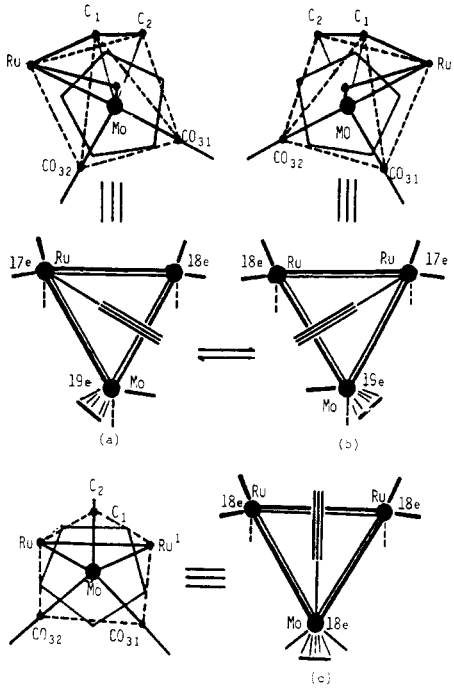

Figure 3. Proposed edge-hopping mechanism of VII showing local electron counts.

move, the overall motion of the molecule must traverse a symmetrical intermediate in order to simultaneously exchange the two CO's on Mo and the six CO's on the two rutheniums.

One would think that, when the *tert*-butylacetylido group moves, it could also σ-bond to the Mo atom. This symmetrical structure seems reasonable, especially if one recalls that it complies with the EAN rule precisely (not only would the trimetallic cluster as a whole have 48 electrons, but also the local electron counts would also be 18 for all three metal atoms (Figure 3). Yet, both the solid-state structure and the solution spectra after heating show no evidence for this structure in the ground state. Although the spectroscopic experiments do not rigorously exclude this structure as an intermediate, we do not think that it is obtained since the preference of cyclopentadienylmolybdenum(I) complexes is to exist as a square-based pyramid configuration. In other words, if the *tert*-butylacetylene group σ-bonded to Mo and bisected the Ru–Ru edge of the metal triangle, the Mo would have to adopt a pentagonal-based pyramidal structure. To our knowledge, such a structure has not been observed in any of the molybdenum(I) complexes with similar ligands. We cannot rigorously exclude intermetallic scrambling between the two Ru atoms in VII, but this process alone would not simultaneously average the two carbonyls on the Mo atom. Studies exploring the generality of the photolysis reaction which forms VII with other mixed-transition-metal mercury clusters are currently under way.

Experimental Section

Materials. $[Ru_3(\mu_3\text{-}\eta^2\text{-}C_2\text{-}t\text{-}Bu)(CO)_9](\mu\text{-}HgI)$ was synthesized by known literature procedures[1-4] from $Ru_3(CO)_{12}$ which was purchased from Strem Chemicals. $[Mo(\eta^5\text{-}C_5H_5)(CO)_3]_2$ from Strem Chemicals was used as received. Triphenyl- and trimethylphosphine were both ACS reagent grade, the former purchased from Aldrich Chemical Co. and the latter from Strem Chemicals.

All solvents were reagent grade. Tetrahydrofuran and cyclohexane were distilled from sodium–benzophenone ketyl under nitrogen prior to use. Other solvents were stored over molecular sieves and saturated with inert gas before use.

Silica gels for preparative column and thin-layer chromatography were both from E. Merck (PF 254-60). Analytical TLC was performed with Eastman sheets (number 13181 with fluorescent indicator).

^{13}CO-enriched $Ru_3(CO)_{12}$ and $[Mo(\eta^5\text{-}C_5H_5)(CO)_3]_2$ were prepared by equilibrating the compounds with 0.5 atm of 90% ^{13}CO at 90 °C in heptane for 4–5 days. The enriched compounds were recrystallized from toluene.

Spectra and Analyses. Both KBr solid and CH_2Cl_2 solution infrared spectra were recorded on a Nicolet-20 DXB FT-infrared spectrometer. NMR spectra were measured on a IBM NR/80 spectrometer. For ^1H NMR, samples were dissolved in degassed $CDCl_3$ except for the studies of the redistribution reaction of phosphine-substituted I where C_6D_6 was used to achieve better separation of signals. Variable-temperature ^{13}C NMR spectra were recorded in CD_2Cl_2 and $CD_3C_6D_5$. Chromium acetylacetonate (0.05 M) was added to ^{13}C NMR samples as a relaxation agent. ^{31}P NMR spectra were obtained in chloroform solution with $CDCl_3$ added to provide an internal field-frequency lock. ^{31}P NMR chemical shifts were referenced to internal triphenylphosphine which was referenced to external H_3PO_4 by using a value of 6.0 ppm.

Carbon and hydrogen analyses were performed by Schwarzkopf Microanalytical Laboratories, New York, NY. Spectroscopic data and elemental analysis results for all the compounds reported are given in Table I.

Preparation of I. The preparation below is a slightly modified version of the published procedure.[2] $[Mo(\eta^5\text{-}C_5H_5)(CO)_3]_2$ (216 mg, 0.44 mmol) was dissolved in 100 mL of freshly distilled tetrahydrofuran in a 100-mL Schlenk tube, and the solution was degassed with N_2 for at least 5 min. Under strict nitrogen atmosphere, about 0.2 mL of Na–K alloy was syringed into the above solution with a flame-dried syringe. The purple solution was then stirred under N_2 until it turned to a light yellow color, which took about 3–4 h. Stirring was then stopped, and the solution was allowed to stand an additional 5 h to settle particles of unreacted metal and any other insolubles. $[Ru_3(\mu_3\text{-}\eta^2\text{-}C_2\text{-}t\text{-}Bu)(CO)_9](\mu\text{-}HgI)$ (771 mg, 0.08 mmol) was dissolved in a minimum volume of THF in a 250-mL round-bottom flask and the solution degassed with N_2. Both solutions were cooled in an ice bath, and then the clear yellow solution of Mo^- combined via cannulation, with stirring. As soon as the cannulation was completed, the solvent was removed under vacuum. The residue taken up in methylene chloride was then separated by preparative TLC using a 1:4 mixture of CH_2Cl_2/hexanes as eluent. Three bands were eluted, the top and bottom band being identified as II and III, respectively. The middle band was collected and recrystallized from hot hexanes. Dark orange crystals (476 mg) of $[Ru_3(\mu_3\text{-}\eta^2\text{-}C_2\text{-}t\text{-}Bu)(CO)_9](\mu_3\text{-}Hg)[Mo(\eta^5\text{-}C_5H_5)(CO)_3]$ (I) were obtained (55% yield).

Thermolysis of I. Compound I (50 mg, 0.05 mmol) was dissolved in 50 mL of solvent (THF or heptane) and the solution degassed with N_2. The solution was refluxed while N_2 gas was slowly bubbled through it. The reaction was followed by analytical TLC. Appearance of II was observed in about 1 h. After 15 h, the $HRu_3(C_5H_5)(CO)_9$ and $[Mo(\eta^5\text{-}C_5H_5)(CO)_3]_2Hg$ started to appear. Reflux was stopped after 20 h. The solvent was then removed by rotary evaporation, and the reaction mixture was separated by preparative TLC, with a 1:4 mixture of CH_2Cl_2/hexanes as eluent. All four bands, including the starting material as the major band, were collected. Yields are presented in eq 1.

Photolysis of I. I (50 mg, 0.05 mmol) was dissolved in about 100 mL of benzene in a water-cooled photolysis chamber. While a slow flow of N_2 was maintained, the solution was irradiated with ultraviolet light from a Hanovia quartz mercury lamp (140 w). The reaction was monitored by TLC. The color of the solution turned brown in a few minutes and continued to become darker while the product band appeared and grew on the TLC plate. The reaction was stopped when all starting material was consumed, which took 2 h in a quartz reaction chamber and about 4 h in a Pyrex glass chamber. After rotary evaporation, the reaction mixture was separated by preparative TLC with a 1:4 mixture of CH_2Cl_2/hexanes as eluent. There were many bands, and a double elution was necessary to give a clear separation of major bands. In addition to the major product band, there were minor bands assignable to $Ru_3(CO)_{12}$, $HRu_3(C_6H_9)(CO)_9$, $[Ru_3(\mu_3\text{-}\eta^2\text{-}C_2\text{-}t\text{-}Bu)(CO)_9]_2(\mu_4\text{-}Hg)$ (II), $[Mo(\eta^5\text{-}C_5H_5)(CO)_3]_2Hg$ (III), and

$[Mo(\eta^5\text{-}C_5H_5)(CO)_3]_2$, based upon TLC, IR, and NMR analyses; three other minor bands are yet to be identified. The crude major product band was isolated in 20% yield before recrystallization from hot hexanes.

Phosphine Substitution on I. In a typical procedure 100–200 mg (0.1–0.2 mmol) of I was dissolved in 50–100 mL (THF, cyclohexane, or heptane) of solvent, and a 10% molar excess of trimethyl- or triphenylphosphine was added. In all cases, a flow of N_2 was passed slowly through the solution to keep the solution free of oxygen and, also, to reduce the partial pressure of dissociated CO to speed up the substitution reaction. The progress of the reaction was monitored by analytical TLC. Since the starting material I was never consumed completely, reaction was stopped when there was no further product formation based on TLC (20–36 hours). After rotary evaporation, the reaction mixture was separated with preparative TLC. While I could be best separated from triphenylphosphine with plain hexanes or a 1:4 mixture of CH_2Cl_2/hexanes, IV and V had to be separated from one another with a 2:3 mixture of CH_2Cl_2 and hexanes. Therefore TLC had to be performed twice to separate all the components from each other. The bis-substituted product VI was crystallized from hot hexanes to yield bright orange granules (10–15% based on I). IV was isolated as a yellow-orange solid (15–20% based on I). The solubility of V was much lower than of IV. Analytical data and spectroscopic data used to identify the phosphine-substituted products can be found in Table II.

Redistribution Reaction of IV with V. IV (11.5 mg) was weighed into a clean, dry NMR tube. V (11.5 mg) was weighed into another NMR tube of the same quality. Degassed deuteriated benzene, C_6D_6 (0.4 mL), was syringed into each of the NMR tubes. N_2 was immediately run over the surface of the solution in each tube to purge out residual air, this operation being done for an identical length of time for each sample. Whereas IV dissolved relatively easily, V required slight warming to complete the solution process. A "single pulse" ^1H NMR spectrum was recorded for each sample under the same conditions as for the entire experiment in order to make sure that both samples were pure and unchanged. With two identical 0.5-mL syringes, 0.2 mL of the IV solution and 0.2 mL of the V solution were transferred simultaneously into a third clean, dry NMR tube. A single pulse was run immediately after the solutions of IV and V were mixed and every 10 min thereafter. The intensities of both the cyclopentadienyl resonances and the *tert*-butyl resonances for the two mono-substituted derivatives started to decrease, and, at the same time, resonances appeared and started to increase in intensity for VI, the bis-substituted derivative, and for I, the unsubstituted $[Ru_3(\mu_3\text{-}\eta^2\text{-}C_2\text{-}t\text{-}Bu)(CO)_9](\mu_3\text{-}Hg)[Mo(\eta^5\text{-}C_5H_5)(CO)_3]$. In about 2 h the spectra stopped changing. Signals arising from $HRu_3(C_6H_9)(CO)_9$ and from $[Ru_3(\mu_3\text{-}\eta^2\text{-}C_2\text{-}t\text{-}Bu)(CO)_9]_2(\mu_4\text{-}Hg)$ were not seen until at least 24 h after mixing. Integrations for each of the four resonances arising from the *tert*-butyl group in I, IV, V, and VI in the reaction were averaged over the time period between 2 and 4 h after the mixing. The four averaged integration values were substituted into the following equation to estimate the equilibrium constant

$$K_{eq} = (I_1I_6)/(I_4I_5)$$

where I_1, I_6, I_4, and I_5 represent the integrations for I, VI, IV, and V, respectively, in the equilibrated mixture.

Protonation of I, IV, V, and VI. Samples of I, IV, V, or VI (20–30 mg) were dissolved in 0.5 mL of CD_2Cl_2 in a 5-mm NMR tube. Trifluoroacetic acid (0.1–0.2 mL) was added to the solutions and the ^1H NMR of the solutions recorded at 1-h intervals for 5–6 h. In the case of IV and VI broad hydride signals were observed at −18.3 to −18.5 ppm which are typical shifts for μ-hydrides on an Ru_3 cluster. In the case of I and V only small downfield shifts of the hydrocarbon ligand resonances are observed. In none of the above cases was the hydride resonances at −5.4 ppm associated with $HMo(C_5H_5)(CO)_3$ seen.

X-ray Data Collection and Reduction. Suitable crystals of VII for diffraction study were obtained by recrystallization of the compound in hexane. A yellow rectangular sample was secured to the tip of a thin glass fiber with epoxy and mounted on a goniometer. Data were collected at room temperature (~23 °C) on a Nicolet $P2_1$ four-circle diffractometer equipped with a graphite monochrometer and Mo X-ray source. A total of 15 reflections ($12° < 2\theta < 25°$) well distributed in reciprocal space were selected from rotation photographs and machine centered. Accurate unit cell parameters obtained from least-squares treatment of the orienting reflections along with data collection parameters are summarized in Table III. From unit cell constants and systematic extinctions ($h0l$, $l = 2n + 1$; $0k0$, $k = 2n + 1$) the space group was uniquely determined as monoclinic, $P2_1/c$ (C_{2h}, No. 14). Data were corrected for Lorentz and polarization effects, and an empirical absorption correction was applied (relative transmission factors varied between 0.86 and 1.00). The absorption correction was performed by using the ψ-scan technique. Equivalent sets of data were merged (R_{int} = 1.3%) to give 3854 unique reflections. All data reduction was performed with the local program PROCESS. Instrumental and crystal stability was monitored with three selected standards ($54\bar{2}$; 400; 402) measured every 50 reflections. Only random statistical fluctuations (<3%) were observed in their intensities over the period of data collection.

Table V. Positional and Thermal Parameters[a] for $Ru_2Mo(CO)_8(\mu_3\text{-}C_2\text{-}t\text{-}Bu)(\eta^5\text{-}C_5H_5)$

atom	x	y	z	B/B_{eq}, Å^2
Ru(1)	0.32547 (3)	0.68351 (1)	0.70530 (1)	2.388 (6)
Ru(2)	0.37815 (3)	0.51852 (1)	0.76462 (2)	2.635 (7)
Mo	0.12941 (3)	0.61596 (1)	0.79670 (1)	2.157 (6)
C(11)	0.2646 (4)	0.7956 (2)	0.6644 (2)	3.43 (8)
O(11)	0.2373 (3)	0.8625 (1)	0.6395 (2)	3.43 (8)
C(12)	0.5118 (4)	0.7171 (2)	0.7965 (2)	3.89 (9)
O(12)	0.6213 (3)	0.7395 (2)	0.8500 (2)	6.05 (9)
C(13)	0.4242 (4)	0.6652 (2)	0.6171 (2)	4.09 (9)
O(13)	0.4840 (4)	0.6537 (2)	0.5640 (2)	7.53 (11)
C(21)	0.5559 (4)	0.5288 (2)	0.8718 (2)	3.91 (9)
O(21)	0.6591 (3)	0.5381 (2)	0.9361 (2)	5.94 (9)
C(22)	0.4956 (4)	0.4808 (2)	0.6903 (2)	3.70 (9)
O(22)	0.5620 (3)	0.4565 (2)	0.6453 (2)	6.23 (9)
C(23)	0.3311 (4)	0.4093 (2)	0.7952 (2)	4.29 (10)
O(23)	0.3043 (4)	0.3427 (2)	0.8103 (3)	7.61 (11)
C(31)	0.0983 (4)	0.7385 (2)	0.7870 (2)	3.41 (8)
O(31)	0.0698 (3)	0.8081 (1)	0.7881 (2)	5.20 (8)
C(32)	0.3179 (4)	0.6430 (2)	0.9014 (2)	3.74 (9)
O(32)	0.4133 (3)	0.6600 (2)	0.9678 (2)	5.59 (8)
C(1)	0.1903 (3)	0.5662 (2)	0.6770 (2)	2.45 (6)
C(2)	0.0923 (3)	0.6260 (2)	0.6412 (2)	2.35 (6)
C(3)	−0.0409 (3)	0.6512 (2)	0.5584 (2)	2.77 (7)
C(4)	−0.1606 (4)	0.5800 (3)	0.5336 (3)	3.99 (9)
C(5)	−0.1200 (4)	0.7313 (2)	0.5742 (2)	3.80 (9)
C(6)	0.0230 (5)	0.6649 (3)	0.4794 (2)	4.25 (10)
C(7)	0.0485 (4)	0.5624 (3)	0.9143 (2)	4.55 (10)
C(8)	−0.0617 (4)	0.6189 (2)	0.8651 (3)	4.36 (10)
C(9)	−0.1283 (4)	0.5872 (2)	0.7762 (2)	3.85 (9)
C(10)	−0.0559 (5)	0.5100 (2)	0.7734 (3)	4.42 (10)
C(14)	0.0514 (5)	0.4948 (2)	0.8582 (3)	4.79 (11)
H(41)	−0.205 (6)	0.569 (3)	0.583 (3)	5.4
H(42)	−0.243 (6)	0.593 (3)	0.478 (3)	5.4
H(43)	−0.120 (6)	0.535 (3)	0.521 (4)	5.4
H(51)	−0.048 (6)	0.779 (3)	0.589 (3)	5.0
H(52)	−0.205 (6)	0.742 (3)	0.521 (3)	5.0
H(53)	−0.164 (6)	0.723 (3)	0.620 (3)	5.0
H(61)	−0.071 (6)	0.677 (3)	0.426 (3)	5.3
H(62)	0.070 (6)	0.619 (3)	0.469 (3)	5.3
H(63)	0.089 (6)	0.717 (3)	0.491 (3)	5.3
H(7)	0.111 (6)	0.567 (3)	0.974 (3)	5.3
H(8)	−0.092 (6)	0.665 (3)	0.882 (3)	5.0
H(9)	−0.196 (6)	0.609 (3)	0.730 (3)	5.2
H(10)	−0.070 (6)	0.476 (3)	0.722 (4)	5.4
H(14)	0.120 (6)	0.441 (3)	0.877 (3)	5.7

[a] The esd's given in parentheses refer to the least significant digits. $B_{eq} = {}^4/_3\sum\beta_{ij}a_{ij}$. The isotropic temperature factors for the hydrogen atoms have the assigned value equal to 1.5 + C_{iso}(riding).

Structure Solution and Refinement. The positions of the three heavy atoms were located from a Patterson map. A trial structure phased with the metal atom positions resulted in an R factor of 20%. The following difference Fourier synthesis led to the positions of the remaining non-hydrogen atoms. The coordinates of the C_p carbon atoms confirmed the positional assignment of Mo. The atomic coordinates and thermal parameters (isotropic followed by anisotropic) were refined by full-matrix least squares,[10] minimizing the function $\sum w(|F_o| - |F_c|)^2$, where

$w = 1/\sigma^2(F_o)$. A difference Fourier map calculated in the final stages of refinement revealed the positions of all hydrogen atoms in the structure. These were included in the final cycles of refinement with isotropic temperature factors set at $H_{iso} = [1.5 + C_{iso} - H]$. Neutral atomic scattering factors and anomolous dispersion corrections for Ru and Mo atoms used were those tabulated in ref 11. The R indices and refinement parameters are given in Table III. The final positional and thermal parameters of VII are listed in Table V, and selected interatomic distances and angles are given in Table IV. A complete listing of the observed and calculated structure factor amplitudes, anisotropic thermal parameters, and bond distances and angles are available as supplementary material.

(10) CRYGLS, local crystallographic least-squares program. All computational work was performed on the CDC-Cyber 170/760 at the State University Data Center, Los Angeles, CA, and CSULA.
(11) Cromer, D. T.; Waber, J. T. *International Tables for X-Ray Crystallography*; Kynoch: Birmingham, England, 1974; Vol. IV, Table 2.2A. Cromer, D. T. *Ibid.* Table 2.3.1.

Acknowledgment. We gratefully acknowledge the National Science Foundation (CHE-8412047) for support of this research.

Registry No. I, 84802-27-7; II, 84802-26-6; III, 12194-13-7; IV, 112840-69-4; V, 112840-70-7; VI, 112840-72-9; VII, 112840-71-8; $[Mo(\eta^5\text{-}C_5H_5)(CO)_3]_2$, 12091-64-4; $[Ru_3(\mu_3\text{-}\eta^2\text{-}C_2\text{-}t\text{-}Bu)(CO)_9](\mu\text{-}HgI)$, 74870-35-2; $HRu_3(C_5H_5)(CO)_9$, 72942-48-4; $HRu_3(C_6H_9)(CO)_9$, 57673-31-1; $Ru_3(CO)_{12}$, 15243-33-1.

Supplementary Material Available: Anisotropic thermal parameters (Table VI) and bond distances and angles (Table VII) (4 pages); a complete listing of the observed and calculated structure factor amplitudes (17 pages). Ordering information is given on any current masthead page.

Metal to Ligand Charge-Transfer Photochemistry of Metal–Metal Bonded Complexes. 5.† ESR Spectra of Stable Rhenium–α-Diimine and Spin-Trapped Manganese–α-Diimine Radicals

Ronald R. Andréa, Wim G. J. de Lange, Tim van der Graaf, Marcel Rijkhoff, Derk J. Stufkens,* and Ad Oskam

Anorganisch Chemisch Laboratorium, Universiteit van Amsterdam, J.H. van't Hoff Instituut, Nwe Achtergracht 166, 1018 WV Amsterdam, The Netherlands

Received August 20, 1987

Irradiation ($\lambda \geq 320$ nm) of $(CO)_5MM'(CO)_3L$ and $Ph_3SnM'(CO)_3L$ (M, M' = Mn, Re; L = α-diimine = 2,2′-bipyridine, 1,10-phenanthroline, pyridine-2-carbaldehyde imine, and 1,4-diaza-1,3-butadiene) leads to homolysis of the metal–metal bond yielding fairly stable solvated radicals $SM'(CO)_3L^\bullet$. These paramagnetic species have been studied by ESR spectroscopy in solution directly or by using nitroso-2,2-dimethylpropane as a spin-trapping reagent. The ESR spectra show extensive hyperfine splittings of the unpaired electron with the nuclei ^{14}N, ^{1}H, and ^{55}Mn or $^{185,187}Re$. From the observed and computer-simulated coupling constants important information could be derived about the electronic structure of the singly occupied molecular orbital (SOMO). After in situ addition of $P(OPh)_3$, $P(OMe)_3$, or pyridine (= L′) to $Re(CO)_3(t\text{-Bu-DAB})^\bullet$, the new paramagnetic adducts axial-$(L')Re(CO)_3(t\text{-Bu-DAB})^\bullet$ could be identified.

Introduction

For many years organometallic reactions have been assumed to proceed via intermediates with 16 or 18 valence electrons.[1] Recently, however, many reactions have been found in which 17- or 19-valence-electron complexes are involved as intermediates.[2,3]

Thus, several ligand substitution reactions have been found to proceed much more rapidly when a small (anodic or cathodic) current was passed through the solution.[2] Alternatively, 17-electron metal-centered radicals such as $M(CO)_5$, $M(CO)_4L$, $M(CO)_3L_2$ (M = Mn, Re), $CpM'(CO)_3$ (M′ = Mo, W), $CpFe(CO)_2$, and $Co(CO)_4$ have been prepared photochemically, mainly from their metal–metal bonded dimers.[3-7] Several of these radicals have been identified as intermediates using transient spectroscopic techniques[8] or as persistent radicals in solutions or low-temperature matrices.[9] Substitution reactions of 17-electron species provided kinetic evidence for associatively activated pathways with formation of 19-electron species as intermediates.[3,9e,10] Further evidence for the formation of these 19-electron intermediates was provided by the electron-transfer reactions of these radicals.[3,5-7,11] Espe-

†For part 4, see: Andréa, R. R.; de Jager, H. E.; Stufkens, D. J.; Oskam, A. *J. Organomet. Chem.* **1986**, *316*, C24.

(1) Tolman, C. A. *Chem. Soc. Rev.* **1972**, *1*, 337.
(2) Kochi, J. K. *J. Organomet. Chem.* **1986**, *300*, 139.
(3) Stiegman, A. E.; Tyler, D. R. *Comments Inorg. Chem.* **1986**, *5*, 215.
(4) Geoffroy, G. L.; Wrighton, M. S. *Organometallic Photochemistry*; Academic: New York, 1979.
(5) Meyer, Th. J.; Caspar, J. V. *Chem. Rev.* **1985**, *85*, 187.
(6) Stiegman, A. E.; Tyler, D. R. *Coord. Chem. Rev.* **1985**, *63*, 217.
(7) Stiegman, A. E.; Tyler, D. R. *Acc. Chem. Res.* **1984**, *17*, 61.
(8) (a) Yesaka, H.; Kobayashi, T.; Yasafuku, K.; Nagakura, S. *J. Am. Chem. Soc.*, **1983**, *105*, 6249. (b) Rothberg, L. J.; Cooper, N. J.; Peter, K. S.; Vaida, V. *J. Am. Chem. Soc.* **1982**, *104*, 3536. (c) Hughey, IV, C. J. L.; Anderson, C. P.; Meyer, Th. J. *J. Organomet. Chem.* **1977**, *125*, C49. (d) Herrick, R. S.; Herrinton, T. R.; Walker, H. W.; Brown, T. L. *Organometallics* **1985**, *4*, 42. (e) Hanckel, J. M.; Lee, K.; Rushman, P.; Brown, T. L. *Inorg. Chem.* **1986**, *25*, 1852. (f) Freedman, A.; Bersohn, R. *J. Am. Chem. Soc.* **1978**, *100*, 4116. (g) Bray, R. G.; Seidler, P. F., Jr.; Gethner, J. S.; Woodin, R. L. *J. Am. Chem. Soc.* **1986**, *108*, 1312. (h) Seder, T. A.; Church, S. P.; Weitz, E. *J. Am. Chem. Soc.* **1986**, *108*, 7518. (i) Poliakoff, M.; Weitz, E. *Adv. Organomet. Chem.* **1986**, *25*, 277. (j). Moore, B. D.; Simpson, M. B.; Poliakoff, M.; Turner, J. J. *J. Chem. Soc., Chem. Commun.* **1984**, 785. (5) Moore, B. D.; Poliakoff, M.; Turner, J. J. *J. Am. Chem. Soc.* **1986**, *108*, 1819. (l) Waltz, W. L.; Hackelberg, O.; Dorfman, L. M.; Wojcicki, A. *J. Am. Chem. Soc.* **1978**, *100*, 7259. (m) Meckstroth, W. K.; Walters, R. T.; Waltz, W. L.; Wojcicki, A.; Dorfman, L. M. *J. Am. Chem. Soc.* **1982**, *104*, 1842. (n) Junk, G. A.; Svec, H. J. *J. Chem. Soc. A* **1970**, 2102.

0276-7333/88/2307-1100$01.50/0